ISSN 2355-3286

Predictive Control of Speed, Steering, and Braking for An Autonomous Car on Uphill and Downhill Road

Ryan Aditya[1], Ari Santoso[2]
[1,2] Department of Electrical Engineering, Institut Teknologi Sepuluh Nopember, Surabaya, Indonesia
[1]ryn.adty19@gmail.com

Accepted on November 13, 2025
Approved on December 30, 2025

***Abstract*— Countries around the world have roads that go through mountains and hills. These roads can have features such as winding and change of elevation. When passing through such roads, the car's dynamics are influenced by the unknown elevations and curvatures, which can threaten stability if not properly controlled. The purpose of this research is to control the cars longitudinal speed through acceleration, braking through regenerative braking and maintain lateral control through steering inputs. The proposed hierarchical control scheme consists of a high-level predictive controller which predicts the car's dynamics under varying road condition and a low-level Fuzzy-PID controller for the actuators, which is motor driver and electric power steering (EPS). Additionally, the energy recovery from the regenerative braking system is monitored to evaluate its impact on battery state of charge, especially when the car is slowing down or going through downhill roads. The control system proposed aims to maintain speed and steering stability under varying road conditions and improve energy efficiency. The simulation will be done using MATLAB and the car will go through a spiral down track and a U-turn ramp track. The proposed controller manages to track both the cars speed and acceleration under the present of roads curvature and downhill disturbance. The Fuzzy-PID also manage to track the reference generated by the NMPC with a slightly damped response. For the battery state of charge (SOC) there is a rise of 0.0025% or equivalent to 40 Wh generated from regenerative braking.**

***Index Terms*—Autonomous Car; Fuzzy-PID; Predictive Control; Regenerative Braking**

I. INTRODUCTION

An autonomous car is a vehicle that can operate on its own without human intervention. The purpose of autonomous car control research is mainly based on speed, which focuses on longitudinal dynamics and steering control for lateral dynamics. With the growing shift to electric motors and battery-powered systems for cars, more methods are developed for utilizing the motor's excessive mechanical energy by converting it back into electrical energy. This method is called regenerative braking and helps recharge the car's battery during deceleration[1], [2], [3].

The research on autonomous car control has been ongoing for quite a while now. In [4], an adaptive cruise control (ACC) combined with regenerative braking which uses two-layer control is developed. The first control layer consists of an adaptive fuzzy sliding mode control (AFSMC) and a low-level control brake system distribution control, mainly to manage force distribution between mechanical and regenerative brake. The proposed method is capable of accurately tracking the vehicle speed under various road conditions, including wet and dry surfaces.

In [5], the research aims to maintain stability with a combination of both mechanical and regenerative brakes. The proposed controller is a PI controller which output controls determine the ratio between mechanical and regenerative brake used when slowing down. Though this research only focuses on junction type roads. In [6], a sliding mode control (SMC) combined with performance guarantee (PG) was proposed to control the vehicles speed and steering. The PG method aims to keep the vehicle's state errors to converge to zero while constraining it within the determined limit. However, these studies have yet integrated all three elements of speed, steering and braking. Therefore, this study aims to fill that gap by combining these three elements.

Model predictive control (MPC) and its nonlinear variants (NMPC) have been applied extensively to vehicle steering, longitudinal control and integrated braking problems; [7] developed a robust predictive control of an autonomous car steering system for path-tracking using LMI optimization with independent constraints enforcement. Applications of NMPC for collision avoidance path planning and tracking control for autonomous vehicles have been demonstrated in [8]. Regenerative and mechanical brake integration have also been approached with predictive control for performance and energy recovery[9]. Fuzzy–PID and adaptive fuzzy controllers are widely used at actuator level to handle nonlinearities and reduce transient overshoot[10]. Finally, open-source toolchains (CasADi, IPOPT) and commercial environments (MATLAB/Simulink) are commonly used to

implement and test NMPC and the lower-level controllers used here[11], [12], [13].

In this work, we propose a hierarchical control scheme that consist of a high-level predictive control focusing on steering and speed control combined with a low-level Fuzzy-PID for the actuators control. The predictive control aims to achieve stability especially when moving through uphill, downhill, and winding roads while the Fuzzy-PID ensures smooth and precise actuation. When the car is slowing down, energy recovery generated from the regenerative braking and its impact on battery state of charge will also be monitored.

This paper is organized as follows: Section I outlines the background and other research related to autonomous car control. Section II describes the car mathematical model and the proposed controller design. Section III discusses the simulation result, focusing on the car's acceleration and steering control inputs, key state parameters and energy recovery via regenerative braking. Section IV contains the summary and conclusion of our research, while also providing direction for future work.

II. METHODOLOGY

A. Car Dynamic and Kinematic Model

The model provided by [14] captures both the longitudinal and the lateral dynamics, in addition a lateral and yaw angle error will be added to the model. The states will be formulated as follows:

$$x = [\dot{v}_x, v_x, v_y, \dot{\theta}, e_1, e_2, x_{od}]^T, u = [a, \delta]^T \quad (1)$$

$$y = [v_x, e_1, e_2 + x_{od}]^T \quad (2)$$

where $x_1 = \dot{v}_x$ is the longitudinal acceleration; $x_2 = v_x$ is the longitudinal speed; $x_3 = v_y$ is the lateral speed; $x_4 = \dot{\theta}$ is the car yaw angle speed; $x_5 = e_1$ is the lateral deviation; $x_6 = e_2$ is the relative yaw angle; and $x_7 = x_{od}$ is the longitudinal deviation. For the control input $u_1 = a$ and $u_2 = \delta$ are the car acceleration and steering respectively.

The car's longitudinal dynamic is simplified as a first order model, while the lateral dynamic model will contain some nonlinearities affected by the longitudinal speed. The model is described as follows:

$$\dot{x}_1 = \frac{1}{\tau}(-x_1 + u_1 + d_1) \quad (3)$$

$$\dot{x}_2 = x_1 + x_3 x_4 \quad (4)$$

$$\dot{x}_3 = \frac{1}{m}(F_{y12} + F_{y34}) - x_2 x_4 \quad (5)$$

$$\dot{x}_4 = \frac{1}{I_z}\left(l_f F_{y12} - l_r F_{y34}\right) \quad (6)$$

The cars mass and inertia are respectively m and I_z. The cars time constant is denoted as τ. The lateral tire forces are denoted as F_y, where subscripts 1,2 refer to the front tire and 3,4 the rear tire. The tire forces for the front side will be considered equal on both side, this also apply to the rear side. The car wheels distance from the center gravity are l_f for the front wheels and l_r for the rear wheels.

$$F_{y12} = u_2 - C_{af}\frac{x_3 + l_f x_4}{x_1} \quad (7)$$

$$F_{y34} = -C_{ar}\frac{x_3 - l_r x_4}{x_1} \quad (8)$$

The wheels cornering stiffness are denoted as C_a, where the subscripts f, r refer to the front and rear tires. The error model for both lateral and yaw angle deviation are defined accordingly:

$$\dot{x}_5 = x_3 + x_2 x_6 \quad (9)$$

$$\dot{x}_6 = x_4 - x_2 \rho \quad (10)$$

the disturbance term d_1 represents the roads gradient on the longitudinal axis, while ρ denotes the road's curvature value. Finally, the car kinematics will be captured with the bicycle model as follows:

$$\begin{bmatrix}\dot{x}\\ \dot{y}\\ \dot{\theta}\end{bmatrix} = \begin{bmatrix}v\cos\theta\\ v\sin\theta\\ \frac{v}{L}\tan\delta\end{bmatrix} \quad (11)$$

Where θ is the car yaw angle, δ is the steering angle, v is the car speed and L is the distance between the front and back wheel.

B. Nonlinear Model Predictive Control

Model Predictive Control is a feedback digital feedback control method with the ability to predict the system's output within the desired horizon. This prediction is calculated virtually inside the controller based on the system mathematical model and the control output then produced through cost function calculations[15]. Refer to [16], [17] for general MPC references for theory and design.

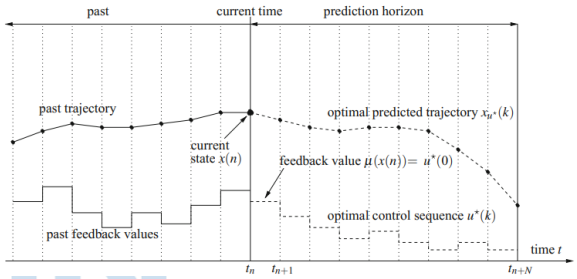

Fig. 1 Nonlinear predictive control scheme

For Nonlinear Model Predictive Control (NMPC), the system model is formulated as:

$$x^+ = f(x, u) \quad (12)$$

where f is the nonlinear function of the model with state x and input u while x^+ indicates the future state value. The predicted state x_u can be obtained by iterating equation (14) between the horizon N.

$$x_u(0) = x(n) \quad (13)$$

$$x_u(k+1) = f\big(x_u(k), u(k)\big), k = 0, \dots, N-1 \quad (14)$$

The control value obtained from the state x_u is then calculated through a cost function formulated as follows:

$$J\big(x(n), u(n)\big) = \sum_{k=0}^{N-1}\|x_u(k)\|^2 + \lambda\|u(k)\|^2 \quad (15)$$

where λ is a weighing value for smooth control command. Constraints can also be used to describe practical hardware limitations. This ensures the optimal control generated by the NMPC is feasible for physical realization. Lastly, the NMPC produce the control sequences necessary based on the prediction N for

every time interval[18]. The NMPC will act as a high-level controller and generate a reference for the actuators to track on.

C. *Fuzzy-PID*

Nonlinearities on practical dynamic systems limit the peformance of a regular PID controllers. Therefore, a PID control can be combined with a fuzzy control scheme to overcome this nonliearities. The gains K_p, K_i, K_d combined with fuzzy logic can now vary depending on the error and error rate of the system[10].

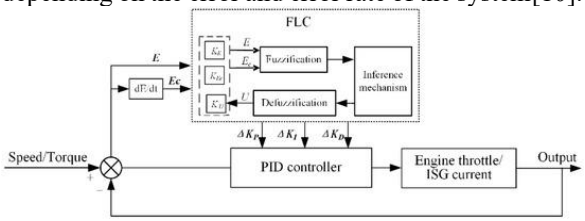

Fig. 2 Example of Fuzzy-PID control scheme

The three main stages of Fuzzy-PID implemantation are; fuzzification, where the error data (typically error and error rate) are mapped into fuzzy sets through the use of membership functions; fuzzy inference, where a rule base system combines the inputs to calculate the fuzzy control values; defuzzification, which converts the fuzzy control back to a crisp tuning of PID gains for final control calculation[19]. The Fuzzy-PID will be in charge of controlling the low-level actuators which are the motor drive for the car speed control and the electric power steering (EPS) for the car steering control.

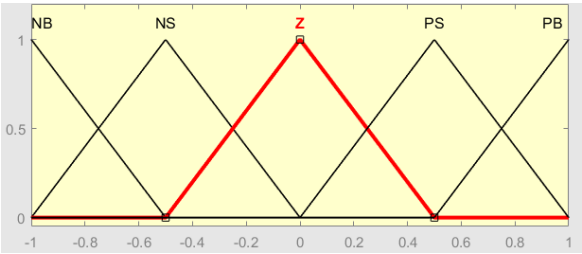

Fig. 3 Input Membership Function Structure Example

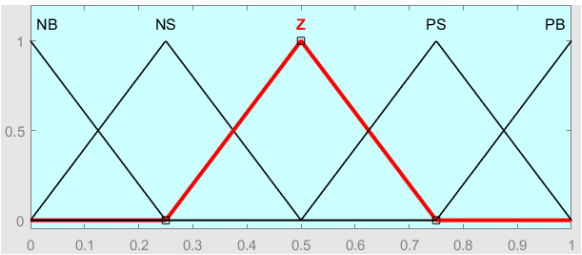

Fig. 4 Output Membership Function Structure Example

For this Fuzzy-PID controller, identical fuzzy membership functions is applied for all PID gain components. Specifically, the membership functions associated with the proportional, integral, and derivative gains are defined with the same number of linguistic terms, uniform widths, and symmetric distributions. This design choice is adopted to maintain consistency of the actuator control and reduce tuning complexity. An example of the input membership functions can be seen in Figure 3. which contains five overlapping fuzzy sets, namely Negative Big (NB), Negative small (NS), Zero (Z), Positive Small (PS), and Positive Big (PB). The same is also applied to the output membership functions shown in Figure 4. Even though the membership functions show similarity, there is a key difference which is the variable range. The input variables (actuators error and error rate) are normalized over the range of $[-1,1]$, this allows the Fuzzy-PID to process both positive and negative error values. In contrast the fuzzy outputs represent scaling factors for the PID gains and constrained to the interval of $[0,1]$, this allows a simpler tuning for each gain since the main proportional, integral and derivatives gain are outside the fuzzy membership functions. The rule sets for each gain are shown on Table 1-3.

TABLE I. PROPORTIONAL GAIN (KP) RULE SET

de/e	NB	NS	Z	PS	PB
NB	PB	PS	Z	NS	NB
NS	PS	PS	Z	NS	NS
Z	Z	Z	Z	Z	Z
PS	NS	NS	Z	PS	PS
PB	NB	NS	Z	PS	PB

TABLE II. INTEGRAL GAIN (KI) RULE SET

de/e	NB	NS	Z	PS	PB
NB	NB	NB	NB	Z	Z
NS	NB	NS	Z	PS	Z
Z	NS	Z	Z	Z	PS
PS	Z	PS	Z	PS	PB
PB	Z	Z	PS	PB	PB

TABLE III. DERIVATIVE GAIN (KD) RULE SET

de/e	NB	NS	Z	PS	PB
NB	NS	Z	PS	PB	PB
NS	Z	PS	PS	PB	PB
Z	PS	PB	Z	PS	PB
PS	PB	PB	NS	Z	PS
PB	PB	PB	NS	Z	NS

TABLE IV. ACTUATOR FUZZ-PID GAINS

Gain	Motor Drive	EPS
Kp	5	15
Ki	1	5
Kd	1	4

D. Energy Recovery

Regenerative braking will be used as the main source of the battery energy recovery. During the regenerative braking the motor will act as a generator, excess kinetic energy will be converted back into electrical energy through electromagnetic torque. The motor in this research will be used for both propulsion and regenerative braking. Therefore, a condition is needed to distinguish propulsion mode and regenerative braking mode. For propulsion mode the conditions are:

$$T_m < T_e \; and \; I_m > 0 \quad (16)$$

and for generator mode:

$$T_m > T_e \; and \; I_m < 0 \quad (17)$$

The electrical and mechanical torque of the motor are denoted as T_m and T_e, while I_m is the motor current. When these conditions are met the battery will be allowed to charge. The battery will only be monitored on charging mode, so the system will be modelled as follows:

$$P_b = \eta_m \eta_p T_m \omega_m \quad (18)$$

and the state of charge (SOC) is modelled as follows:

$$\frac{d}{dt}(SOC) = -\eta_{bchg} \frac{I}{Q_b} \quad (19)$$

$$I = \frac{V_{oc} - \sqrt{V_{oc}^2 - 4R_{int}P_b}}{2R_{int}} \quad (20)$$

Where η_m,η_p,η_{bchg} are respectively the efficiency of the motor, electrical circuit and battery charging. The motor torque and speed are denoted as T_m and ω_m, the battery voltage is V_{oc}, the battery internal resistance is R_{int} and Q_b is the battery capacity[4, 20].

III. Results and Discussion

The simulations are carried out in MATLAB, where the main focus will be steering and speed control. Energy regeneration will also be monitored due to the car slowing down on the downhill road. The track used for simulation will be a downward circle track and U-turn ramp, which will capture both the steering and the disturbance produced by the change of gradient and curving roads. The car system and hierarchical control scheme for the simulation will be constructed as in Figure 5, where the NMPC will act as high-level planner and the Fuzzy-PID will control both the motor and steering actuator. Afterward the output generated by both actuators will be fed into the car model.

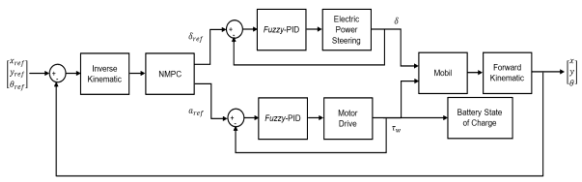

Fig. 5. System block diagram

The sampling time for the NMPC will be 0.1 seconds. The prediction horizon of the NMPC is set to 10 steps ahead and the control horizon 2 steps ahead. There are also some constraints given for the speed (21) and steering control (22) reference that will be given to the actuators as follows:

$$-3 < a < 3 \text{ (m/s)} \quad (21)$$

$$-0.5 < \delta < 0.5 \text{ (rad)} \quad (22)$$

The acceleration constraints represent typical passenger-vehicle acceleration and deacceleration capability without requiring extreme actuator effort. This range also allows normal and reasonably aggressive speed changes. The steering angle constraint refers to the front-wheel steering angle, which is a typical front wheel turning angle. The battery internal circuit will also be considered ideal so the heat generated from it won't affect the battery charging. This assumption helps simplify modelling and reduce computational complexity. Conditions (17) will be used as a basic ON-OFF trigger for charging the battery. Some of the parameters used on the simulation are mentioned in Table 5 and Table 6.

TABLE V. CAR PARAMETERS

Parameter	Value
Mass (m)	1575 (kg)
Moment of inertia (I_z)	2875 ($kg.m^2$)
Front wheels distance (L_f)	1.2 (m)
Rear wheels distance (L_r)	1.6 (m)
Front wheels cornering stiffness (C_{af})	19000 (N/rad)
Rear wheels cornering stiffness (C_{ar})	33000 (N/rad)
Time constant (τ)	0.2 (s)

TABLE VI. BATTERY PARAMETERS

Parameter	Value
Motor efficiency	0.85
Circuit efficiency	0.96
Battery efficiency	0.9
Battery voltage	60%
Battery Capacity	18 kWh
Internal resistance	0.025 (Ω)

A. *Spiral Down Track*

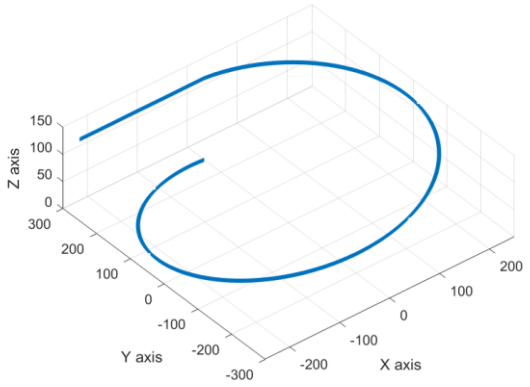

Fig. 6. Spiral down track preview

The track starts with a 250 m straight road as shown in Figure 6. then circling down on a track with 250 m radius. The starting height will be 150 m therefore the car will be going downhill with a slope of 2.7°. The car will try to maintain a constant speed of 8.33 m/s or equivalent to 30 km/h from start until going downhill while doing a turn. The simulation ends after going through a full circular track.

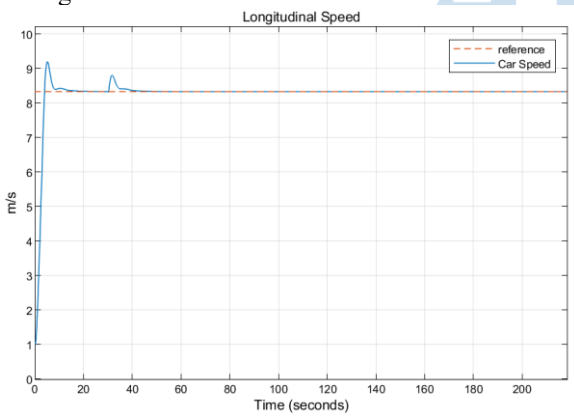

Fig. 7. Spiral down track longitudinal speed

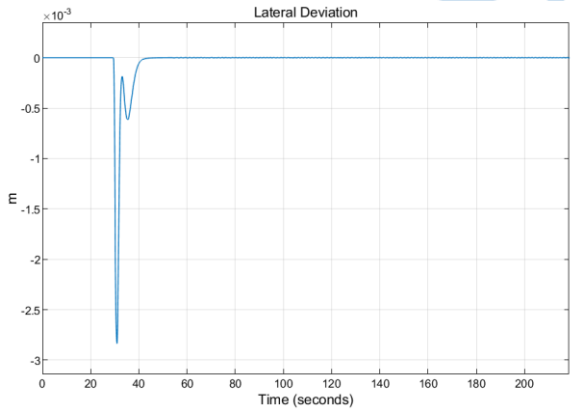

Fig. 8. Spiral down track lateral deviations

Figure 7. presents the car longitudinal speed, where the speed reach around 8.33 m/s on steady-state which is equivalent to 30 km/h. There are two overshoots observed from the simulation result. First is during the initial acceleration with a peak value of around 9% before settling. This can be caused by a small lag between the actuator's responses and the NMPC reference. Integrating the actuator dynamic directly might solved this problem, but the low-level control contains a Fuzzy-PID. Therefore, a new problem arises to integrate the low-level control loop into the NMPC.

The second overshoot occurs when the car starts to turn after going straight for 250 m with a peak value of around 5% before settling again. This overshoot might be caused by the combination of both the road turning and going downward happening at the same time. The lack of smoothness generated from the track waypoints also affects the transient response of the system, causing some minor overshoot along the way.

Figure 8. presents both the lateral deviation throughout the motion. At the start of the turn, the lateral deviation shows a brief negative spike, which indicates that the vehicle initially drifts slightly toward the inside of the curve. This spike is short-lived and is corrected rapidly, the controller brings the deviation back toward zero within around 10 seconds. Such behaviour typically arises from curvature changes. The swift return to near-zero value suggest that the controller maintains stability even under the presents of disturbance.

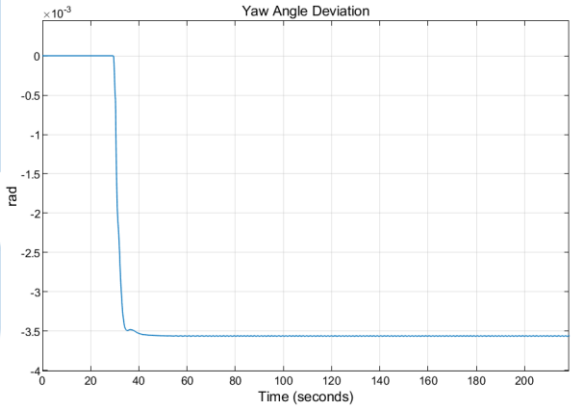

Fig. 9. Spiral down track yaw angle deviations

The yaw angle deviation plot from Figure 9. shows a small but consistent offset between the vehicle's heading and the tangent direction of the track. This indicates that the vehicle follows a slightly different curvature than the reference arc. Even so, the deviation remains very small around the order of 10^{-3} rad, meaning the vehicle's trajectory is effectively parallel to the desired path with only a negligible angular error.

Together, the lateral and yaw angle responses demonstrate that while the vehicle temporarily experiences a small disturbance at the start of the turn, the controller quickly stabilizes the motion and preserves accurate path following. The magnitude of both deviations is extremely small, showing that the proposed controller is capable of maintaining smooth

and stable lateral behaviour even in the present of curvature changes and under the influence of other external factors such as roadway slope.

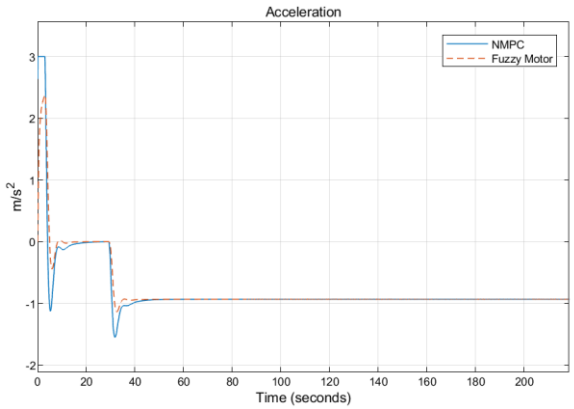

Fig. 10. Spiral down track motor acceleration tracking control

Figure 10. compares the acceleration reference generated from the NMPC (blue line) with the actual acceleration generated by the motor controlled with the Fuzzy-PID (orange-dashed line). The results show that the proposed inner-loop controller is able to track the NMPC reference acceleration with good fidelity, particularly once the acceleration reaches steady-state. During the transient phase, small differences between the reference signal and the actuator response are noticeable. These deviations occur primarily during two key periods: the initial acceleration to the desired speed and when the car start going through a downhill.

At the beginning of the motion, the NMPC demands a relatively high positive acceleration to rapidly bring the vehicle up to the target reference speed. This aggressive command is expected, as the NMPC optimizes speed tracking while respecting the system's constraints. In contrast, the Fuzzy-PID controller damps out excessive acceleration, which result in slightly slower rise in acceleration. Despite this small difference, the vehicle still reaches the desired velocity with minimal overshoot, as confirmed earlier in Figure 5. A similar behaviour occurs when the vehicle goes through a downhill. The NMPC lowers the reference by providing negative acceleration to maintain the desired speed under the effect of the road gradient. The Fuzzy-PID controller once again produce a slightly damped output. Even so, the difference remains small and the actuator consistently converges toward the NMPC output reference once it reaches steady-state.

The close alignment between the two responses in the steady-state region demonstrates effective coordination between the high-level NMPC and the low-level Fuzzy-PID control. The small transient difference does not translate into notable speed tracking errors, indicating that the combined control structure is able to overcome minor delays. In practice, this behaviour is desirable because it prevents excessive torque application, reduces mechanical stress on drivetrain components, and enhances ride comfort.

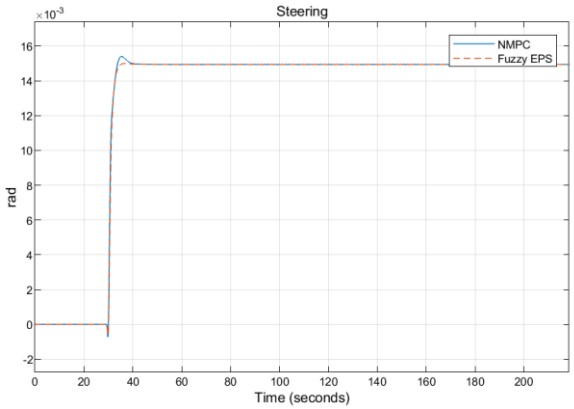

Fig. 11. Spiral down track electric power steering tracking control

The comparison between the NMPC reference (blue line) and the Fuzzy-PID controlled EPS is shown in Figure 11. Both signals converge to a steady-state value of approximately 0.015 rad, which is consistent with the curvature required to follow the reference turn. Although the final values match closely, several important transient characteristics can be observed during the motion. As the vehicle approaches the start of the turn, the steering reference generated by the NMPC contains another brief overshoot, similar to the phenomenon can be seen in the motor acceleration response in Figure 10.

On the actuator side, the Fuzzy-PID controller once again outputs a smoother and more damped steering response. While the NMPC produces another aggressive reference, the Fuzzy-PID for the EPS response slightly slower resulting less overshoot with similar output results. The smoothing effect is beneficial from a practical standpoint, as it reduces mechanical stress on the steering actuator. Once again, despite the small difference between the reference and the EPS steering angle, the EPS output still remains within the NMPC's imposed steering constraint and doesn't produce significant tracking errors. This is also confirmed by the previous lateral and yaw angle deviations shown in Figure 8. and Figure 9. Respectively. Overall, the steering results demonstrate another effective coordination between the NMPC and the Fuzzy-PID controller. The combination leads to stable and accurate path tracking, with the NMPC providing predictive steering command reference and the Fuzzy-PID controller ensures smooth, physically realizable actuation behaviour even when encountering non-smooth waypoints transitions.

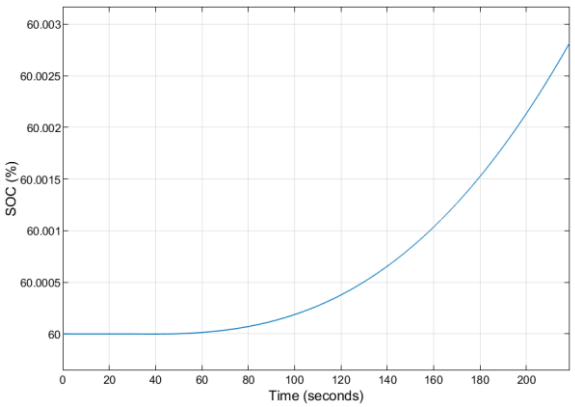

Fig. 12. Spiral down track battery state of charge

Figure 12. illustrates the battery SOC throughout the downhill track of the simulation. Although the absolute change in the battery's SOC is relatively small, the curve indicates a gradual increase in stored energy due to the activation of regenerative braking during the descent. Over 220 seconds of downhill, the SOC rises by approximately 0.0025% relative to its initial state. Based on the battery's nominal capacity and voltage parameters, this amount is equivalent to around 40 Wh of energy. While the value may appear small, it is physically consistent with the limited length of the simulation and the gradient of the slope used on the track in the scenario.

It is important to note that in this research, the model only monitor the charging aspect of the battery and ignore any discharge activity. This assumption allows the SOC curve to represent only the recovered energy, without the cofounding effect of other devices energy draw. As such, the SOC profile shown on Figure 10. should be interpreted as the maximum possible recovery within the defined scenario. Another important note is the integration of mechanical brake has not yet been done in this research. Overall, the soc behaviour confirms that the system responds appropriately to downhill disturbance by converting excess mechanical energy from the motor into stored electrical energy.

B. U-Turn Ramp Track

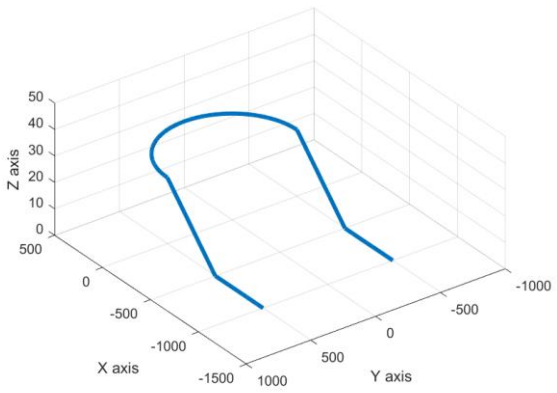

Fig. 13. U-turn ramp track preview

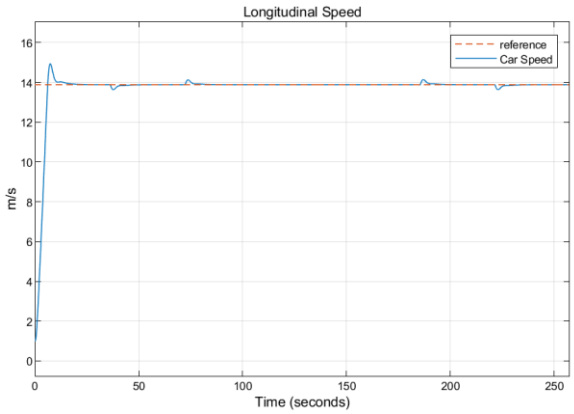

Fig. 14. U-turn ramp track longitudinal speed

For the second experiment, a U-turn combined with a ramp will be used. The track starts and ends with a 500 m straight road as shown in Figure 10. while the turn is half a circle with a radius of 500 m. Both of the ramps will have a length of 500 m and a slope of 2.86°. The car will try to maintain a constant speed of 13.88 m/s or equivalent to 50 km/h from start until finish. This will highlight both the dynamic of going uphill and downhill while also doing a turn. Figure 14. shows the longitudinal speed for the U-turn ramp track, where the speed reach around 13.88 m/s on steady-state which is equivalent to 50 km/h. There are one overshoot and 4 small bumps observed from the simulation result. First is the same during the initial acceleration with a peak value of around 9% before settling. The four overshoots occurs when the car starts and finish going through both downhill and uphill before settling again. This overshoot might be caused by the sudden change of road gradients. The negative small bumps indicate the car slows down, the first small bump is when the car is going uphill and the second one is when the car trying to slow down after going downhill. In the contrast, the positive bumps indicate the cars speeds up due to the change of road gradient, first is after finishing the uphill and later after entering downhill motion. This shows the controller able to counter the effect of road gradients with small errors.

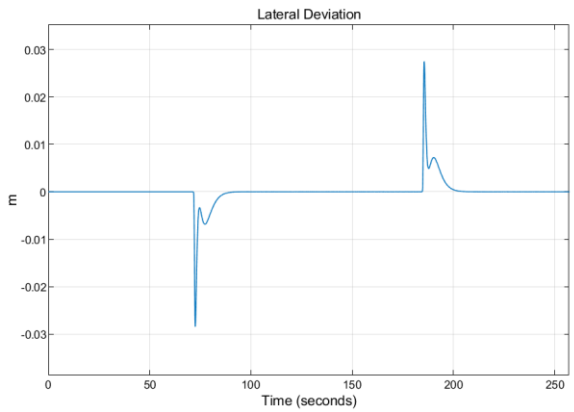

Fig. 15. U-turn ramp track lateral deviation

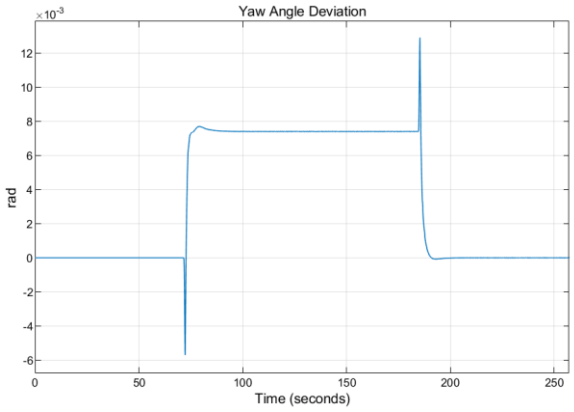

Fig. 16 U-turn ramp track yaw angle deviation

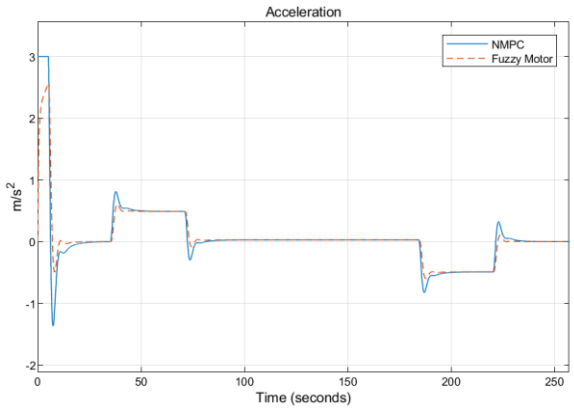

Fig. 17. U-turn ramp track acceleration tracking control

The deviations from Figure 15. and Figure 16. shows the car going through the U-turn segment. Similar spikes show at the start and the end of the turn which can be seen on Figure 8. And Figure 9. before. This is the effect of the non-smooth trajectory generated for the turning motion. Though the deviations are short lived and quickly corrected by the controller. The acceleration tracking for this track is shown in Figure 17. The cars acceleration shows the same profile as the longitudinal speed on Figure 14. There are four bumps each when starting and finishing both downhill and uphill motion. The control scheme still manages to track the acceleration even on the present of the uphill motion. Lastly, the controller also manages to track the cars steering before and after going through an uphill and downhill motion as shown in Figure 18.

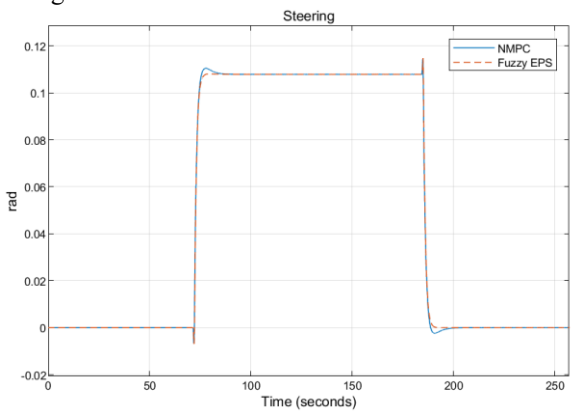

Fig. 18. U-turn ramp track steering tracking control

IV. Conclusion

The hierarchical control scheme—comprising an NMPC high-level planner and Fuzzy-PID low-level actuator controller—successfully maintained vehicle stability through both speed and steering control even under the presence of disturbance such as curving road, uphill road and downhill road. The Fuzzy-PID manages to damp the overshoot generated from NMPC setpoint reference which is likely caused by non-smooth waypoint generation and the absence of actuator dynamics on the NMPC model. The motor is also able to generate a small amount of charge which is 0.0025% or equivalent to 40 Wh. Overall, the results show effective coordination between the NMPC and the Fuzzy-PID. Future work should focus on optimizing waypoint generation for low-jerk trajectories and incorporating actuator dynamics into the NMPC model.

References

[1] P. Saiteja, B. Ashok, A. S. Wagh, and M. E. Farrag, “Critical review on optimal regenerative braking control system architecture, calibration parameters and development challenges for EVs,” Int J Energy Res, vol. 46, no. 14, pp. 20146–20179, Nov. 2022, doi: 10.1002/er.8306.

[2] A. T. Hamada and M. F. Orhan, “An overview of regenerative braking systems,” J Energy Storage, vol. 52, p. 105033, Aug. 2022, doi: 10.1016/J.EST.2022.105033.

[3] Q. Chengqun et al., “A novel regenerative braking energy recuperation system for electric vehicles based on driving style,” Energy, vol. 283, p. 129055, Nov. 2023, doi: 10.1016/J.ENERGY.2023.129055.

[4] J. Guo, W. Li, J. Wang, Y. Luo, and K. Li, “Safe and Energy-Efficient Car-Following Control Strategy for Intelligent Electric Vehicles Considering Regenerative Braking,” IEEE Transactions on Intelligent Transportation Systems, vol. 23, no. 7, pp. 7070–7081, Jul. 2022, doi: 10.1109/TITS.2021.3066611.

[5] C. S. Nanda Kumar and S. C. Subramanian, “Brake force sharing to improve lateral stability while regenerative braking in a turn,” Proceedings of the Institution of Mechanical Engineers, Part D: Journal of Automobile Engineering, vol. 233, no. 3, pp. 531–547, Feb. 2019, doi: 10.1177/0954407017747373.

[6] H. Xia, J. Chen, F. Lan, and Z. Liu, “Motion Control of Autonomous Vehicles with Guaranteed Prescribed Performance,” Int J Control Autom Syst, vol. 18, no. 6, pp. 1510–1517, Jun. 2020, doi: 10.1007/s12555-019-0442-5.

[7] N. N. Nam and K. Han, "Path-tracking Robust Model Predictive Control of an Autonomous Steering System Using LMI Optimization With Independent Constraints Enforcement," Int J Control Autom Syst, vol. 22, no. 11, pp. 3352–3363, 2024, doi: 10.1007/s12555-023-0772-1.

[8] D. Dong, H. Ye, W. Luo, J. Wen, and D. Huang, "Collision Avoidance Path Planning and Tracking Control for Autonomous Vehicles Based on Model Predictive Control," Sensors, vol. 24, no. 16, Aug. 2024, doi: 10.3390/s24165211.

[9] M. Mei, S. Cheng, H. Mu, Y. Pei, and B. Li, "Switchable MPC-based multi-objective regenerative brake control via flow regulation for electric vehicles," Front Robot AI, vol. 10, Feb. 2023, doi: 10.3389/frobt.2023.1078253.

[10] P. Mohindru, "Review on PID, fuzzy and hybrid fuzzy PID controllers for controlling non-linear dynamic behaviour of chemical plants," Artificial Intelligence Review 2024 57:4, vol. 57, no. 4, pp. 97-, Mar. 2024, doi: 10.1007/S10462-024-10743-0.

[11] M. Bloor et al., "PC-Gym: Benchmark Environments For Process Control Problems," Dec. 2024, [Online]. Available: http://arxiv.org/abs/2410.22093

[12] S. W. Jannah and A. Santoso, "Nonlinear Model Predictive Control for Longitudinal and Lateral Dynamic of Autonomous Car," in Proceedings - 11th Electrical Power, Electronics, Communications, Control, and Informatics Seminar, EECCIS 2022, Institute of Electrical and Electronics Engineers Inc., 2022, pp. 145–148. doi: 10.1109/EECCIS54468.2022.9902927.

[13] R. Verschueren et al., "acados—a modular open-source framework for fast embedded optimal control," Math Program Comput, vol. 14, no. 1, pp. 147–183, 2022, doi: 10.1007/s12532-021-00208-8.

[14] R. Rajamani, Vehicle Dynamics and Control, 2nd ed. Berlin: Springer, 2011. doi: 10.1007/978-1-4614-1433-9.

[15] R. C. Rafaila and G. Livint, "Nonlinear model predictive control of autonomous vehicle steering," in 2015 19th International Conference on System Theory, Control and Computing, ICSTCC 2015 - Joint Conference SINTES 19, SACCS 15, SIMSIS 19, Institute of Electrical and Electronics Engineers Inc., Nov. 2015, pp. 466–471. doi: 10.1109/ICSTCC.2015.7321337.

[16] J. B. Rawlings, D. Q. Mayne, and M. M. Diehl, "Model Predictive Control: Theory, Computation, and Design 2nd Edition." [Online]. Available: http://www.nobhillpublishing.com

[17] D. Q. Mayne, J. B. Rawlings, C. V Rao, and P. O. M. Scokaert, "Survey Paper Constrained model predictive control: Stability and optimality."

[18] L. Grüne and J. Pannek, "Communications and Control Engineering Nonlinear Model Predictive Control Theory and Algorithms Second Edition." [Online]. Available: http://www.springer.com/series/61

[19] H. Qin, L. Wang, S. Wang, W. Ruan, and F. Jiang, "A Fuzzy Adaptive PID Coordination Control Strategy Based on Particle Swarm Optimization for Auxiliary Power Unit," Energies 2024, Vol. 17, Page 5311, vol. 17, no. 21, p. 5311, Oct. 2024, doi: 10.3390/EN17215311.

[20] Q. He, Y. Yang, C. Luo, J. Zhai, R. Luo, and C. Fu, "Energy recovery strategy optimization of dual-motor drive electric vehicle based on braking safety and efficient recovery," Energy, vol. 248, p. 123543, Jun. 2022, doi: 10.1016/J.ENERGY.2022.123543.